Iran University of Science and Technology

Automotive Science and Engineering

Journal Homepage: ase.iust.ac.ir

ISSN: 2008-9899

Study of the effect on manufacturing parameters on the fatigue behavior of aluminum engine mounting bracket

Hossein Khalajzadeh[1], Seyed Vahid Hosseini [*1], Alireza Shaterzadeh [1]

[1]Faculty of Mechanical Engineering, Shahrood University of Technology, Shahrood, Iran.

*Corresponding Email Author: v_hosseini@shahroodut.ac.ir

ARTICLE INFO

Article history:

Received : 8 Jun 2024

Accepted: 27 Sep 2024

Published: 21 Oct 2024

Keywords:

Engine mounting bracket

Manufacturing parameters

High cycle fatigue

Fatigue crack propagation

Strength improvement

A B S T R A C T

The engine mounting bracket connects the engine to the car body and plays a key role in reducing vibrations and supporting the engine's weight and dynamic loads. It must be designed to withstand cyclic forces during normal use but fail safely in high-impact situations, like accidents, to minimize damage. This study examines how manufacturing parameters affect the fatigue performance of aluminum engine mounting brackets in cars. According to the staircase-Locati fatigue test results, the relative mean resistance load was measured at 1.24 with a relative scatter of 0.07, placing it in the unsafe operating region for the engine mounting bracket. To address this, a finite element analysis was carried out to identify critical areas on the part and implement modifications to enhance its performance. The crack initiation and growth regions observed during the fatigue tests aligned closely with the critical zones identified in the finite element analysis. Following the modifications and the removal of production defects, a series of experimental tests were conducted to assess the endurance limit. The results indicated that the relative mean resistance load improved to 1.33 with a relative scatter of 0.06, ensuring safe performance under vehicle operating conditions.

1. Introduction

Since 1850, it has been known that metal under repetitive or fluctuating stress will break at a stress far less than the stress required for a single load. Failures that occur under dynamic loading conditions are called fatigue failures, which is probably based on the fact that failures are generally observed only after a long period of operation. There is no obvious change in the structure of the metal that breaks due to fatigue, so that it can be used as evidence to understand the causes of fatigue failure. With the development of the industry and the increase of devices such as cars, airplanes, compressors, turbines, etc., which are subjected to repetitive and vibrational loading, fatigue has become more common, and now it is considered that fatigue is the cause of at least 90% of failures caused by mechanical reasons during work. Fatigue failure

*Corresponding Author
Email Address: v_hosseini@shahroodut.ac.ir
https://doi.org/10.22068/ase.2024.681

[DOI: 10.22068/ase.2024.681]

is dangerous because it occurs without prior knowledge and visibility. Three major factors are always necessary for the occurrence of fatigue failure. These factors include: a large amount of maximum tensile stress, sufficiently large changes or fluctuations in the applied stress, and a large number of applied stress cycles. In addition, there are other variables such as stress concentration, corrosion, temperature, overload, metallurgical structure, residual stresses, and compound stresses that enhance the conditions for fatigue [1].

Based on what has been mentioned, a comprehensive definition for fatigue can be presented: Fatigue is a local and progressive process of permanent structural change in a point or points of the body, which is starts as a result of applying of periodic stress or strain, and after a number of cycles enough to cause cracks or complete failure [2]. Since fatigue is time-dependent, modeling of physical conditions with appropriate mathematical equations to predict fatigue damage is undoubtedly a challenging task. Fatigue damage modeling in machine components needs to consider various parameters such as geometry, metallurgy and loading conditions so that it can be converted into a mathematical equation. The concept of cumulative damage was presented by Pallerman about a hundred years ago, and twenty years later, the rule of linear damage was introduced by Miner, and for many years, design engineers used these rules to predict the fatigue life of parts. Many scientists have developed numerical and experimental methods to predict fatigue life. With development of computer technology and techniques such as the finite element method and residual stress analysis tools, interest in analysis of fatigue life in welded structures has increased. Some of the related activities can be mentioned.
Findley is one of the first researchers who researched multi-axis fatigue [3]. Ning and Hui studied on the asymptotic stress and strain fields surrounding the tip of a stationary plane strain Mode I crack within a viscoplastic material. Their findings indicated that the stress field in proximity to the crack tip is governed by the Hutchinson–Rice–Rosengren (HRR) field, which exhibits a time-dependent amplitude influenced by the loading history [4]. Xiao et al. based on the Lemaitre damage model with changing of the coefficients of damage growth model, expressed the damage growth in terms of the number of cycles and obtained the fatigue life of the material [5]. Ganjiani used a microhardness test to evaluate damage in aluminum. A suitable agreement was observed between the simulation results and the experimental results [6]. Singh and Khan investigated the behavior of fatigue crack growth in materials exhibiting plastic compressibility alongside hardening and hardening-softening-hardening characteristics. Their findings reveal that crucial factors such as the cyclic stress intensity factor range (ΔK), load ratio (R), number of cycles (N), plastic compressibility (α), and material softening play a significant role in influencing this behavior [7]. Wahab et al. experimentally investigated the effect of compressive residual stress caused by preload on fatigue crack growth of aluminum alloys. The results of their research showed that preloading causes fatigue crack growth to be delayed [8]. Giang et al. investigated impact of microstructural characteristics on fatigue crack initiation in forged M3:2 tool steel. Their research specifically points to the influence of the shape, volume fraction, and distribution of both primary and eutectic carbides. They successfully developed a predictive model for the lifecycle of fatigue crack incubation and the growth of short cracks, showing a commendable alignment with experimental results [9]. Similar research was done on 6082-T6 aluminum alloy by Borrego et al. [10]. Zakavi et al. studied three-dimensional linear-elastic fracture mechanics (3D LEFM). Their findings underscore scenarios in which classical linear-elastic fracture mechanics, typically grounded in plane stress or plane strain assumptions, may lead to erroneous conclusions [11]. Matos et al. investigated the fatigue characteristics and micro-mechanism of failure in AlsiMg0.6 alloy used in diesel engine cylinder heads. They obtained the S-N curve for this particular sample and also found that the surface porosity in the region of maximum tensile stress is the most important factor for fatigue crack initiation [12]. Thrilok and Ali investigated the fatigue strength of the engine mounting bracket using static strength. They used finite element

[DOI: 10.22068/ase.2024.681]

simulation and von Mises failure criterion to determine the static [13]. Vinchurkar and Khanwalkar optimized the strength and weight of the engine mounting bracket. By the finite element method, they identified the high and very low stress areas and suggested reducing the thickness of the low stress areas to optimize the weight [14]. Dixon and Mood [15] presented a straightforward method for statistically analyzing data, which aligns with the outlined requirements. It suggests employing the normal approximation of the binomial distribution and determining confidence intervals for both the mean value and standard deviation. In this regard, with the aim of matching the boundary conditions of the laboratory part with the engine block installed in the car, it is evaluated by using the construction of a special fixture for the desired part. Finally, according to the results of the fatigue test as well as the experimental equations, the fatigue life of the engine mounting bracket will be estimated. Santhosh et al. [16] investigated the dynamic behavior and properties of three types of rubber(natural, butyl, and fluorocarbon rubber) that were used as the material of the engine mounting bracket.The input parameters were the engine speed, vibrations at the engine head, and vibrations at the bracket. It was concluded that the material with a high stiffness and damping ratio had better vibration isolation properties. Burr et al. [17] proposed a numerical approach to predict the fatigue life and grace period of the lattice structures produced by the electron beam melting method. They plotted *S–N* curve for each strut in the lattice structure by taking into account the sources of variability. They estimated the fatigue life based on the damage accumulation law. Sabiston et al. [18] investigated the fatigue life of the injection-molded composite specimens taken from the flat plaque and automotive oil pan. The tension-tension and fully reversed loads were used during the fatigue tests at the room and elevated temperatures. Since the interface stress between the fiber and resin is the main cause failure in the composite part, the fatigue tests were performed with the maximum interface stress and a micromechanics-based model was proposed to obtain the fatigue life in these kinds of parts. Bao et al. [19] used artificial intelligence techniques to predict fatigue life in the selective laser melted Ti-6Al-4 V alloy. A model was proposed to investigate the effects of defect size, location, and morphology on fatigue life. The defect properties were obtained using the postmortem examination and X-ray tomography methods. An error of 1% was observed between the estimated and experimentally measured fatigue life. Hu et al. [20] studied the effects of defects in the microstructure of Ti–6Al–4V material on its fatigue life. They characterize the size, location, and population of the defects using X-ray tomography and estimated the fatigue life by combining them with the fatigue crack propagation model. The critical defect was found, and the stress intensity factor was obtained in its extended defect zone. It was concluded that the fatigue life of the specimen with deeper defects was higher than parts with shallow ones. Serrano-Munoz et al. [21] investigated the torsional fatigue life and crack growth modes of A357-T6 cast aluminum alloy using the surface crack monitoring devices. They used fractographic postmortem and synchrotron tomography equipment to investigate the crack initiation and growth mechanisms in the surface and subsurface regions of the part. Results showed that the new cracks were initiated to grow in mode II on the free surface of the part and the inward propagation is arrested in the early stages of crack initiation.

According to what was discussed in the research background, several papers have been published in the field of analysis of the engine mounting bracket. Most of these studies have been performed using only finite element analysis in static conditions. Meanwhile, the engine mounting bracket is used to isolate the engine vibrations and consequently is under dynamic loading. Few studies have experimental data, which can only be used for a specific engine mounting bracket with specific geometry, loading, and boundary conditions. Therefore, in the present paper, numerical and experimental approaches were applied to investigated the Peugeot engine mounting bracket under fatigue loading. Besides, the performance of this engine mounting bracket, which is made of aluminum, is investigated using static and exceptional loads. The PSA procedure is also employed to estimate the fatigue strength of the part through the staircase method. To increase the reliability of the

[DOI: 10.22068/ase.2024.681]

part, the high-stress areas that need modifications. Finally, the fatigue tests were re-performed on the modified bracket to check its strength and endurance limit. It can be stated that one of the main novelties of the present paper is improvement of the fatigue strength of engine mounting bracket with identifying critical points of the manufactured part and making recommendations for improving the production process, without adding amount of material to the part.

2. Methodology

Since the engine mounting bracket plays an essential role in the car, it must be designed and built in such a way that it has high fatigue resistance. In order to assess the fatigue life of the engine mounting bracket, it is imperative to conduct fatigue tests along the Z axis direction [22]. The initial measure, with the purpose of positioning the engine mounting bracket appropriately with repeatability and securing the engine mounting bracket throughout the test, is required. Therefore, the fixture was designed according to the geometry of the part and the requirements of the test. VCN 150 was used to make the main body of the fixture to perform the test in the Z direction due to its good strength, rust resistance and initial hardness of about 35 Rockwell C. The dimensions of the fixture are designed and built according to the dimensions of the device and the work piece. Subsequently, the fatigue test was conducted on the engine mounting bracket employing an Instron 8802 hydraulic servo machine proudly manufactured in England, possessing a remarkable capacity of 250 kN. The dynamometer sensor used is 25 kN manufactured by Instron, which is shown in Figure 1.

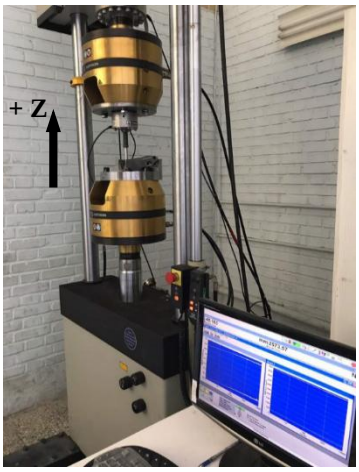

Figure 1. Fatigue test with Instron machine in Z direction.

This assessment is conducted in two phases:

2.1. Primary Locati test

This test is used to find the breaking force of the piece. The fatigue force that will be applied to this part in the car is in the range of $F_n = 2500\,N$ tensile and compressive. Therefore, in the first step, $F_n = \pm 2500\,N$ was selected. In each step, the piece is loaded up to 3×10^5 cycles. If there is no fracture or crack in the piece, the F_n force is increased by 10%, then the test is repeated. When a failure occurs in the part or a crack is observed in the part, this test is completed. The amount of force obtained from this test is used to start the staircase test. This test is performed only once on the piece.

2.2. Secondary staircase and Locati test

In the staircase test [23], the failure force obtained from the primary Locati test is applied to the piece up to $N_{ref} = 10^6$ cycles. The possible state of the piece under test will be in two ways:

a) If the part remains healthy and without any defects until the end of the test, the secondary test of Locati is repeated on the part with an increase of 10% force up to 10^6 cycles and this process continues until the failure of the part; for the next

[DOI: 10.22068/ase.2024.681]

piece, the above steps are repeated with a 10% force increase up to 10^6 cycles.

b) If a crack or fracture is observed in the part during the test, the staircase test is stopped and the next part is tested with a 10% reduction in force and repeating the above process.

In Figure 2 the steps of staircase and Locati test presented.

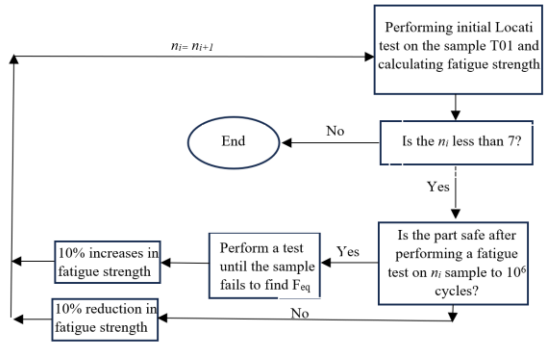

Figure 2. Flowchart of staircase and Locati test.

The basis of the Locati test is the calculation of fatigue resistance based on Basquin's law. After completing the fatigue tests, Basquin's equation was used to express the relationship between the amplitude of the oscillating load and the number of fatigue life cycles as follow: [24]

$$A = NS^b \quad (1)$$

In equation 1, N is the number of load cycles and S is the amplitude of the oscillating load. Also, A and b are material constants. Finally, by completing equation 1 with Pallerman and Miner's linear damage law, as well as the results obtained from the secondary Locati test, the load equivalent to fatigue resistance is calculated by equation 2 [25,26].

$$F_{eq} = \left(\sum_i^n \frac{N_i}{N_{ref}} F_i^b\right)^{\frac{1}{b}} \quad (2)$$

After obtaining the load equivalent to the fatigue resistance of the tested samples from equation 2, finally the average relative resistance (m^*) and relative dispersion (q^*) are calculated using equations 3 and 4 [27].

$$m^* = \frac{\mu}{F_{ref}} = \frac{1}{n\,F_{ref}} \sum_i^n F_{e_i} \quad (3)$$

$$q^* = \frac{\sigma}{F_{ref}} = \frac{1}{(n-1)\,F_{ref}} \sqrt{\sum_i^n (F_i - \mu)^2} \quad (4)$$

The parameters μ and σ refer correspondingly to the mean and standard deviation of the fatigue resistance load. It is also worth noting that F_{ref} symbolizes the initial fatigue force, which should ideally be closely aligned with the anticipated mean fatigue strength, standing at 2500 N, also n represented number of tested samples.

3. Prototype test

The preliminary Locati test was performed with a force of 2500 newtons on the prototype. This test, after 4 stages of increasing force up to 300000 cycles and without any failure of the prototype, finally failed in the 5th stage with a force of 3500 newtons. Table 1 shows the preliminary Locati test results for the prototype (T01 sample). Based on Table 1, the value of $F_{eq}^* = \frac{F_{eq}}{F_{ref}} = 1.30$ was obtained, and the force value obtained from this test is used to start the staircase test. In this Table, normalized force is $F^* = F/F_{ref}$, that F is applied force at each stage of loading.

Table 1. Results of preliminary Locati test to find first value of staircase test

5	4	3	2	1	Number of Load
0.21	0.3	0.3	0.3	0.3	N (Mc)
1.4	1.3	1.2	1.1	1.0	F^*

[DOI: 10.22068/ase.2024.681]

After the preliminary Locati test was finished, a staircase test was taken from 7 other samples. This test shows the failure of parts in different forces, which is shown in Table 2.

Table 2. Results of staircase test. (×:Broken part, ○: Non damaged part)

F*			Test number
1.3	1.2	1.1	
×			T02
	○		T03
×			T04
	×		T05
		○	T06
	×		T07
		○	T08

Finally, with the aim of obtaining the failure force in the pieces left over from the staircase test, the secondary Locati test was performed on the unbroken samples. Based on the results obtained from the secondary Locati test which is shown in Table 3, the average resistance of the samples was calculated as 1.24 with a relative dispersion of 0.07 applied force in the car.

Table 3. Results of secondary Locati test

F_{eq}	Step 2		Step 1		Test number
	F^*	N(Mc)	F^*	N(Mc)	
1.28	1.4	-	1.3	0.90	T02
1.31	1.3	0.39	1.2	1.00	T03
1.30	1.4	-	1.3	1.00	T04
1.19	1.3	-	1.2	0.97	T05
1.22	1.2	0.49	1.1	1.00	T06
1.16	1.3	-	1.2	0.82	T07
1.13	1.2	0.12	1.1	1.00	T08

According to the results obtained after the completion of the fatigue tests, these results were evaluated as unacceptable based on Table 4. This means that the manufactured sample is unsafe.

Table 4. Acceptable range for 6 to 8 tests [28].

Maximum acceptable (q^*)	m^*
0.05	1.2
0.06	1.3
0.07	1.4

3.1. Investigating early causes of failure of the prototype

In order to investigate the early failure, a meeting was held with the presence of the manufacturer and the reasons for the failure were discussed and the reasons for the failure are reported in Figure 3.

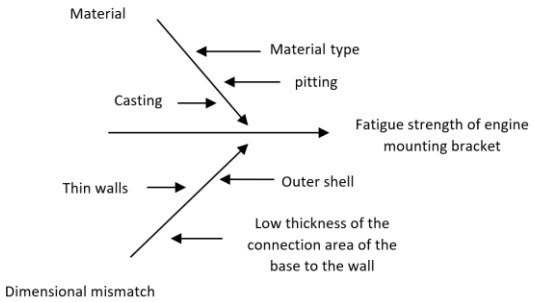

Figure 3. Factors affecting the weakness of the prototype.

After the poor results of the samples in the fatigue test, the reasons for the failure of the samples in the fatigue test will be investigated.

3.1.1. Finite element modeling

Finite element modeling was performed to compare the conditions of the engine mounting bracket under static loading.

Figure 4 shows the modeled sample in finite elements software under tensile and compressive loading. According to Figure 4 and Table 5, the location of stress concentration points and the amount of displacements in these two cases indicate very good agreement. Based on the results, three critical regions were identified, that the most critical state is A and the least dangerous area is C. But in the fatigue test results, the sample fails at location C.

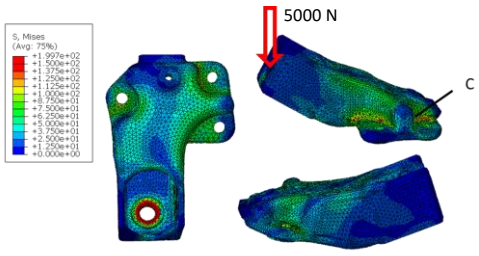

(a) Tension

[DOI: 10.22068/ase.2024.681]

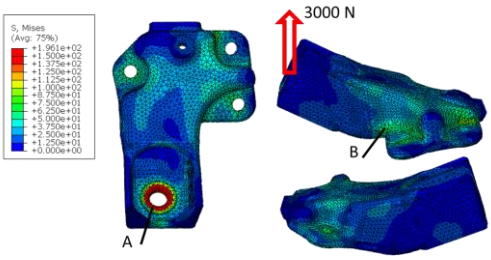

(b) Compression

Figure 4. Finite element modeling of the part.

Table 5. Comparison of experimental and numerical results of the sample.

	Displacement (mm)	Difference (%)	Displacement (mm)	Difference (%)
Experiment	0.5	-	-0.74	-
FEM	0.52	4%	-0.72	2%

3.1.2. Material

The part is made of AL-Si alloy with code A-S7 G03 Y33. The mechanical properties of the part are given in Table 6.

Table 6. Mechanical properties of material.

190 MPa	Yield stress
270 MPa	Ultimate strength
80 HB	Hardness
1	Ultimate strain

The part is produced according to ASTM E155 standard, by sand casting method and without heat treatment. According to ASTM E155, ¼ inch shrinkage holes in wall area shall following with class 4. Accordingly, the part can only be allowed to have one defect in the wall area. Also, in the area of the bases, according to ASTM E155 standard, ¾ inch shrinkage holes must follow with class 5, therefore, in this area, a maximum of four defects are acceptable. In the meeting held, the manufacturer reported that the samples produced were based on the ASTM E155 standard, so the reason for the failure of the samples cannot be the material. During the report presented in the meeting, the presence of burr in the shoulder fillet was observed due to casting. Accordingly, in order to fix this defect, an angle grinder was used, which caused the formation of a groove and the area of stress concentration in B area of the part. Therefore, with the aim of preventing the formation of the stress concentration area in the modified sample, a die grinder was used. In order to investigate more precisely the causes of cracks in the piece, the piece was cut from the connection area of the base to the wall with a wire-cut machine. As shown in Figure 5, pitting was observed in the cut area, which may be due to the presence of sand in the casting mold.

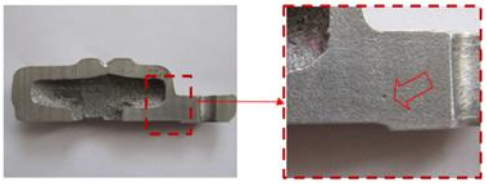

Figure 5. Presence of cavity in the inner wall area.

According to the ASTM E155 standard, after the machining of the part, the presence of holes up to 6 holes in the part with a maximum distance of 10 mm and a maximum depth of 2 mm cannot be the reason for failure in the part. As it is clear in Figure 6, it was observed that the crack did not occur in the connection area of the base to the wall due to the presence of a hole in this area.

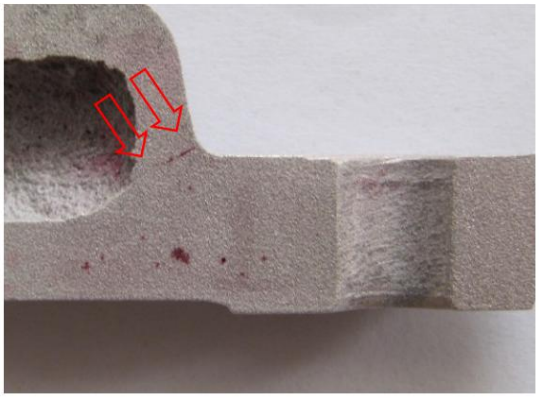

Figure 6. Crack in the inner area of the connection of the base to the wall.

[DOI: 10.22068/ase.2024.681]

3.1.3. Dimensional non-compliance

In order to investigate the reasons for the failure of the prototype in the external shell, a 3D scan was prepared by an optical device made by the Spanish company Nub 3D with a 1.5-megapixel camera lens. Also, the obtained data was entered in the SolidWorks software for the purpose of 3D modeling, which is shown in Figure 7. Finally, with the investigation, it was found that the outer shell of the initially produced part matches with the main designer of the part, so the outer shell of the part cannot be the cause of failure. After examining the outer shell, the thickness of the wall of the produced part was examined by the ultrasonic device made by the American company Olympus, model 38DL-Plus. After obtaining the thickness of the produced part, it was found that in some parts of the wall, such as point 16, the ultrasonic device shows less thickness, but referring to the reports after the test, no cracks were observed in these parts. As shown in Figure 8, the low thickness in these parts cannot be the reason for failure in the part.

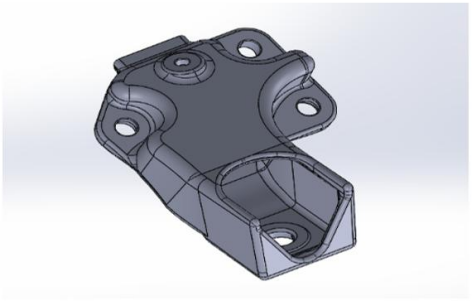

(b)

(a)

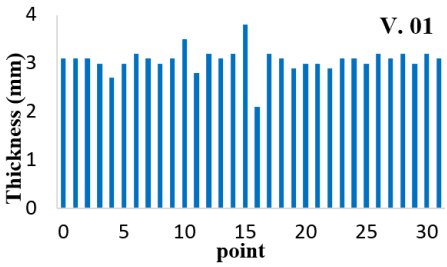

(b)

Figure 7. a) 3D scanning of the external shell with an optical device. b) preparation of a 3D model of the external shell of the prototype in SolidWorks software.

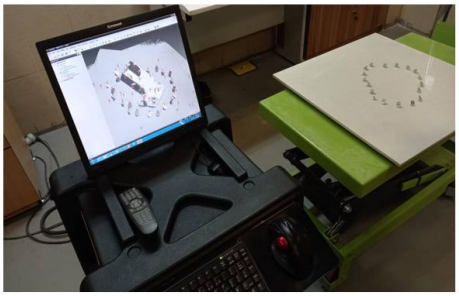

(a)

[DOI: 10.22068/ase.2024.681]

(c)

Figure 8. a) Ultrasonic thickness measurement. b) The graph obtained from the thickness measurement results of the prototype. c) Location of point 16 (Minimum thickness).

Also, using a non-destructive radiographic test by an X-ray machine model DK-2300 made in Denmark, it was observed that the connection area of the base to the wall is prone to yielding and crack growth due to its lower thickness, as shown in Figure 9.

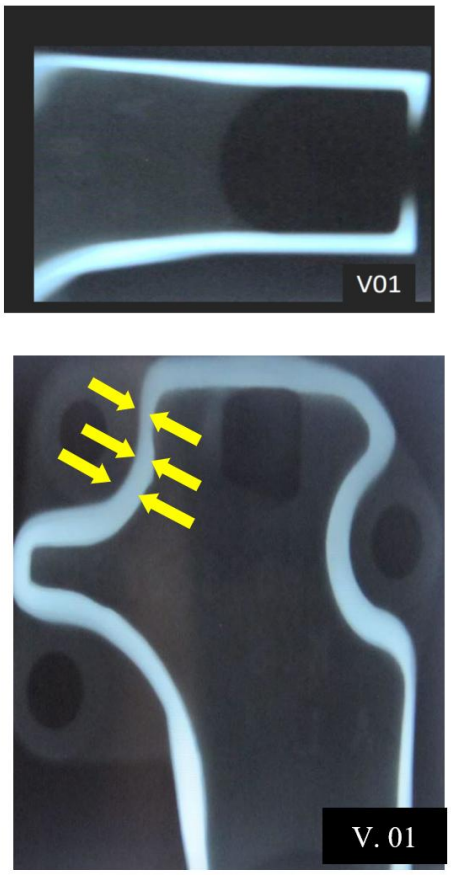

Figure 9. Radiographic image of the prototype.

4. Modified specimen fatigue test

After examining the reasons for the failure of the samples in the high-cycle fatigue test, during the negotiations with the manufacturer, the manufacturing defects that led to the weakness of the part were removed, and the thickness in the critical area was increased by 20%. Before starting the fatigue test again on the modified sample, due to the high cost of the fatigue test, radiographic and thickness measurement tests were performed using non-destructive tests as shown in Figure 10.

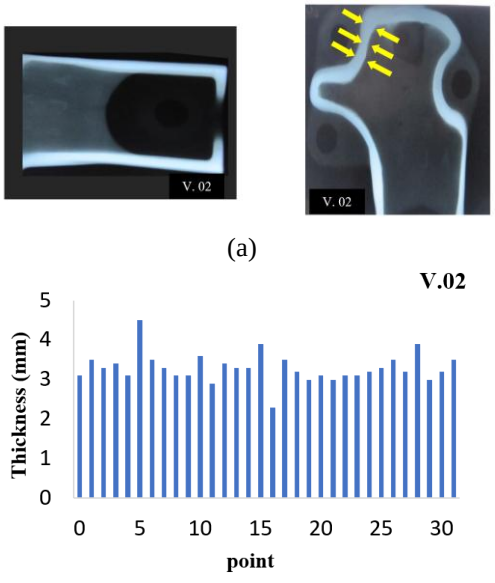

(a)

(b)

Figure 10. a) Radiographic image of the modified sample. b) Graph obtained from thickness measurement of the modified sample.

Then it was found that the thickness in other places has increased by 9%, therefore, 2 grams have been added to the total weight of the secondary sample.

[DOI: 10.22068/ase.2024.681]

Finally, the high-cycle fatigue test was performed again on the modified samples. The method of performing the test on the modified samples is the same as the first test. Like the previous test, in the first stage, a preliminary Locati test was performed with a force of 2500 N on the prototype. In this test, the modified sample, after 4 stages of increasing force up to 300000 cycles and no failure, finally failed in the 5th stage with a force of 3500 N. Based on Table 6, the value of $F_d^* = 1.32$ was obtained, which is used to start the staircase test from the force obtained of this test.

Table 6. The results of the primary Locati test on the modified sample (T01)

5	4	3	2	1	Number of Load
0.29	0.3	0.3	0.3	0.3	N (Mc)
1.4	1.3	1.2	1.1	1.0	F*

After the preliminary Locati test was finished, a staircase test was taken from 6 other samples. This test shows the failure of parts in different forces, which is shown in Table 7.

Table 7. Staircase test results on modified samples.

F*			Test number
1.4	1.3	1.2	
	○		T02
×			T03
	○		T04
×			T05
	×		T06
		○	T07

Finally, with the aim of obtaining the failure force in the pieces left over from the staircase test, the secondary Locati test was performed on the unbroken modified samples. Based on the results obtained from the secondary Locati test which is shown in Table 8, the average resistance of the samples was calculated as 1.33 with a relative dispersion of 0.06 of the applied force in the car. According to the obtained results and based on Table 4, these results were evaluated as acceptable. This means that the modified sample, unlike the first produced sample, has acceptable safety.

Table 8. The results of the secondary Locati test on the modified samples.

F_{eq}	Step 2		Step 1		Test number
	F*	N(Mc)	F*	N(Mc)	
1.43	1.4	0.50	1.3	1.00	T02
1.27	1.5	---	14	0.57	T03
1.38	1.4	0.25	1.3	1.00	T04
1.32	1.5	---	1.4	0.71	T05
1.27	1.4	---	1.3	0.89	T06
1.28	1.3	0.29	1.2	1.00	T07

5. Discussion

The reinforcement of the connection area of the base to the wall in the modified sample has led to the removal of the crack in this area. In order to make a more detailed investigation, after the completion of the fatigue test, a comparison of the primary and secondary samples was made by conducting a penetrating liquid test. Also, after fixing the manufacturing parameters to cause the cracks in the part, by repeating the high-cycle fatigue test on the modified sample, the crack moved from the connection area of the base to the wall to the end area of the part, as shown in Figure 11. This means that similar to the finite element results in the modified sample, the most critical region is located at point A. Table 9 shows the improvement of the modified sample respected to primary sample. As observed, the resistance of modified sample increased by 7% and scatter of fatigue results has decreased by 14%.

[DOI: 10.22068/ase.2024.681]

(a)

(b)

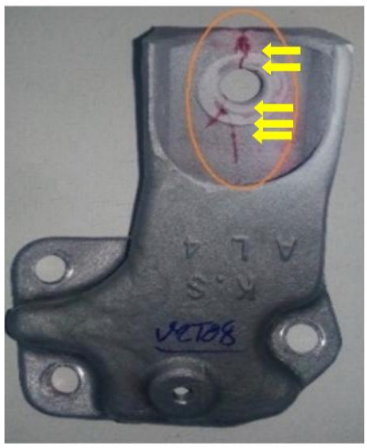

(c)

Figure 11. a) Identification of the crack in the front area of the primary sample. b) Removal of the crack in the front area of the modified sample. c) Appearance of a crack in the end area of the modified sample.

Table 9. The comparison of results of primary and modified samples.

	m*	q*
First Sample	1.24	0.07
Modified Sample	1.33	0.06
Improvement	7%	-14%

6. Conclusion

In the present paper, numerical and experimental approaches were applied to investigated the Peugeot engine mounting bracket under fatigue loading. Besides, the performance of this engine mounting bracket, which is made of aluminum, is investigated using static and exceptional loads. The PSA procedure is also employed to estimate the fatigue strength of the part through the staircase method. To increase the reliability of the part, the high-stress areas that need modifications. The long-cycle fatigue life of the Peugeot car engine mounting bracket was investigated based on cumulative damage. Based on the fatigue tests performed on the prototype, the average resistance of the prototype was 1.24 with a dispersion of 0.07 applied force in the car, which results in unsafe working conditions. During the investigations of the prototype, it led to the fixing of the manufacturing parameters during the production of the part. By repeating the fatigue tests on the secondary samples, the results indicated an increase in the average fatigue resistance up to 1.33 and a dispersion of 0.06 times the applied force, which will be an acceptable performance and safety for the Peugeot car engine mounting bracket. It can be stated that one of the main novelties of the present paper is improvement of the fatigue strength of engine mounting bracket with identifying critical points of the manufactured part and making recommendations for improving the production process, without adding amount of material to the part.

References

[1] G. E. Dieter, Mechanical Metallurgy, 3rd ed., Mc Graw-Hill Co., New York, 375-380, 1986.

[2] ASTM, Annual book of ASTM standards: Fatigue, Philadelphia, E206, 3, 1984.

[DOI: 10.22068/ase.2024.681]

[3] W. N. Findley, "Fatigue of metals under combinations of stresses", 79, 1337-1348, 1957.

[4] Ning, Jing, and Chung Yuen Hui. "Crack tip fields in a viscoplastic solid: monotonic and cyclic loading", International journal of fracture 175, 39-51, 2012.

[5] Y.C. Xiao, S. Li and Z. Gao, "A continuum damage mechanics model for high cycle fatigue", International Journal of Fatigue, 20(7), 503-508, 1998.

[6] M. Ganjiani, "Identification of damage parameters and plastic properties of an anisotropic damage model by micro-hardness measurements", International Journal of Damage Mechanics, 22(8), 1089-1108, 2013.

[7] Singh, Shushant, and Debashis Khan. "On fatigue crack growth in plastically compressible hardening and hardening–softening–hardening solids using crack-tip blunting", International Journal of Fracture, 213(2),139-155, 2018.

[8] M. Wahab, G. Rohrsheim, and J. Park, "Experimental study on the influence of overload induced residual stress field on fatigue crack growth in aluminium alloy", Journal of Materials Processing Technology, 153, 945-951, 2004.

[9] Giang, N. A., U. A. Ozden, A. Bezold, and C. Broeckmann. "A model for predicting crack initiation in forged M3: 2 tool steel under high cycle fatigue", International Journal of Fracture, 187,145-158, 2014.

[10] L. Borrego, J. Ferreira, J. P. Da Cruz and J. Costa, "Evaluation of overload effects on fatigue crack growth and closure", Engineering Fracture Mechanics, 70(11), 1379-1397, 2003.

[11] Zakavi, Behnam, Andrei Kotousov, and Ricardo Branco. "Overview of three-dimensional linear-elastic fracture mechanics." International Journal of Fracture,1-16, 2022.

[12] J. Mattos, A. Uehara, M. Sato and I. Ferreira, "Fatigue properties and micromechanism of fracture of an AlSiMg0.6 cast alloy used in diesel engine cylinder head", Procedia Engineering, 2(1),759-765, 2010.

[13] H. Thrilok and H. Ali, "Using finite element analysis to study the static structural and fatigue life of engine mounting bracket", International Journal of Engineering and Management Research (IJEMR), 5(3), 370-373, 2015.

[14] S. Vinchurkar and P. Khanwalkar, "A review on optimization of engine mounting bracket", International Journal of Engineering Trends and Technology, 35(1), 47-49, 2016.

[15] Dixon, Wilfrid Joseph, and Am M. Mood, "A method for obtaining and analyzing sensitivity data", Journal of the American Statistical Association, 43(241), 109-126, 1948.

[16] Santhosh S, Velmurugan V, Paramasivam V, Thanikaikarasan S, “Experimental investigation and comparative analysis of rubber engine mount vibration and noise characteristics”, Mater Today Proc, 21, 638-642, 2020.

[17] Burr A, Persenot T, Doutre P-T, “A numerical framework to predict the fatigue life of lattice structures built by additive manufacturing”, Int J Fatigue, 139, 105769, 2020.

[18] Sabiston T, Li B, Kang J, “Accounting for the microstructure in the prediction of the fatigue life of injection moulded composites for automotive applications”, Compos Struct, 255, 112898, 2021.

[19] Bao H, Wu S, Wu Z , “A machine-learning fatigue life prediction approach of additively manufactured metals”, Eng Fract Mech, 242,107508, 2021.

[20] Hu YN, Wu SC, Wu ZK, “A new approach to correlate the defect population with the fatigue life of selective laser melted Ti–6Al–4V alloy”, Int J Fatigue, 136, 105584, 2020.

[DOI: 10.22068/ase.2024.681]

[21] Serrano-Munoz I, Shiozawa D, Dancette S, “Torsional fatigue mechanisms of an A357-T6 cast aluminium alloy”, Acta Mater, 201,435-447, 2020.

[22] Beaumont, Pauline, Fabrice Guérin, Pascal Lantieri, Matteo L. Facchinetti, and Guy Martin Borret. "Accelerated Fatigue Tests for reliability estimation of chassis parts", In 2013 Proceedings Annual Reliability and Maintainability Symposium (RAMS), IEEE,1-7, 2013.

[23] D. Radaj, Design and analysis of fatigue resistant welded structures. Woodhead Publishing, 1990.

[24] O.H. Basquin, " The exponential law of endurance tests", proceedings of the ASTM, 30, 625, 1919.

[25] A. Palmgren, Die lebensdauer von kugellagern, "The fatigue life of ball-bearings", Zeitschrift des Vereins Deutscher Ingenieure, 68, 339-341, 1924.

[26] M. A. Miner, "Cumulative damage in fatigue", Journal of Applied Mechanics, 12, A159-A164, 1945.

[27] M. L. Facchinetti, "Fatigue tests for automotive design: optimization of the test protocol and improvement of the fatigue strength parameters estimation", Procedia Engineering, 133, 21-30, 2015.

[28] Pierre V, Pierrick S, Regis M, “Power train adaptation fatigue validation test procedure for metallic parts”, PSA Peugeot-Citroen Stand No B32 0730, 2005.

[DOI: 10.22068/ase.2024.681]